J Mater Sci (2011) 46:1551–1556
DOI 10.1007/s10853-010-4960-z

Novel organic monotectic alloy and its thermal, physicochemical, and microstructural studies

K. P. Sharma · R. N. Rai

Received: 30 July 2010 / Accepted: 28 September 2010 / Published online: 15 October 2010

Abstract The phase diagram study of an organic analogue of a nonmetal–nonmetal system involving 4-bromochlorobenzene and resorcinol shows the formation of a eutectic and a monotectic. The phase equilibrium shows the large miscibility gap region with the consolute temperature 143.0 °C. Growth kinetics of the eutectic, the monotectic and the pure components studied at different undercooling, suggests the applicability of Hillig–Turnbull's equation. For binary materials and parent compounds, the heat of mixing, entropy of fusion, roughness parameter, interfacial energy and excess thermodynamic functions were calculated from the enthalpy of fusion values determined by the DSC method. The solid–liquid interfacial energy shows the applicability of Cahn's wetting condition. The effects of solid–liquid interfacial energy on solidification behaviour of monotectic alloy have also been discussed. The microstructures of monotectic and eutectic show the uniform array of droplets and broken lamella, respectively.

Introduction

The desires of human for variety of materials, for different applications, are becoming wider and demand newer materials of specific properties and of economic cost. The preferred molecule can be synthesized by choosing the parent compounds of specific nature as well as by choosing their interesting composition. The interactions among the constituent molecules result in newer binary materials with changed properties. The binary materials such as metallic eutectics [1, 2], monotectics [3, 4], and intermetallic compounds [5, 6] constitute an established field of investigation in metallurgy and materials science. But due to high transformation temperature, density driven convection effect, opacity, fewer choices of materials etc., they are not suitable for detailed study. The organic materials, similar to metallic systems [7–9], are more scoped due to low transformation temperatures, minimized density driven convection effects and wider choice of materials and also provide an opportunity of direct observation of phase-transformation phenomena. In addition, these materials have been found for nonlinear optical, electronic, and various optoelectronic applications [10–12]. A number of research groups have been prompted to consider organic systems, which are analogues of metallic and non-metallic systems [13–15], as model systems for study in detail. The monotectic systems with liquid phase immiscibility have been studied very less and the mystery of miscibility gap is still unanswered. Therefore, the exploration for more and more binary organic materials as well as monotectic system seems to be worthwhile.

In the present investigation, binary organic system involving 4-bromochlorobenzene (BCB)–resorcinol (R) system have been selected. These materials have high enthalpy of fusion values and could be simulated as organic analogue of nonmetal–nonmetal system. The details of studies concerning phase diagram, linear velocity of crystallization, heat of fusion, Jackson's roughness parameter, interfacial energy, excess thermodynamic functions, and microstructural studies of BCB–R system have been reported.

K. P. Sharma · R. N. Rai (✉)
Department of Chemistry, Banaras Hindu University, Varanasi 221005, India
e-mail: rn_rai@yahoo.co.in

K. P. Sharma
Department of Chemistry, Butwal Multiple Campus, Tribhuvan University, Butwal, Nepal

Experimental

Materials and purification

Resorcinol (Thomas Baker, India) was purified by crystallization from hot water while 4-bromochlorobenzene (Aldrich, Germany) was purified by recrystallization from methanol. The melting temperatures of BCB and R were found to be 65.0 and 110.5 °C, respectively, which are fairly close to their reported values [15, 16].

Phase diagram

The phase diagram of BCB–R system was established in the form of temperature—composition curve [16, 17]. The mixtures of two components, covering the entire range of compositions, were prepared and these mixtures were homogenized by repeating the process of melting followed by chilling in ice cooled water for several times. The melting points of completely miscible compositions and the miscibility temperatures of mixtures showing miscibility gap were determined using a melting point measuring apparatus attached with a precision thermometer of accuracy ±0.5 °C.

Enthalpy of fusion

The values of heat of fusion of the pure components, the eutectic and the monotectic were determined [18, 19] by differential scanning calorimeter (Mettler DSC-4000 system). Indium sample was used to calibrate the system and the amount of test sample and heating rate were about 7.0 mg and 10 °C min^{-1}, respectively, for each estimation. The values of enthalpy of fusion are reproducible with in ±1.0%.

Growth kinetics

The growth kinetics of BCB–R system was studied at different undercoolings by measuring the rate of movement of the solid–liquid interface in U-shaped thin glass tube with about 150 mm horizontal portion and 5 mm internal diameter [15]. The molten sample, pure component/eutectic/monotectic, were separately taken in U-tube and placed in a silicone oil bath. The temperature of oil bath was maintained using microprocessor temperature controller of accuracy ±0.1 °C. At different undercoolings, a seed crystal of the same composition was added to start nucleation, and the rate of movement of the solid–liquid interface was measured using a travelling microscope and a stop watch.

Microstructure

Microstructures of the pure components, the eutectic and the monotectic were recorded by placing a drop of molten compound on a hot glass slide [16]. A cover slip was glided over the melt and it was allowed to solidify unidirectionally. The slide was placed on the platform of an optical microscope (Leitz Labourlux D). The different regions were viewed and interesting regions were photographed with suitable magnification of camera attached with the microscope.

Results and discussions

Phase diagram

The phase diagram of BCB–R system, established between compositions and their melting/miscibility temperatures, shows the formation of a monotectic and a eutectic as depicted in Fig. 1. Melting point of R is 110.5 °C and it decreases on the addition of BCB. When the mole fraction of BCB reaches 0.11, the immiscibility between the melts of BCB and R appears and at a certain temperature these two liquids become completely miscible. With an increase in composition of BCB, the miscibility temperature also increases and attains a maximum value when the mole fraction of BCB reaches 0.50. This maximum temperature is known as the upper consolute/critical temperature (T_c) is 143.0 °C which is 35.0 °C above the monotectic horizontal (M_h). The both components are miscible in all proportions above this critical temperature. The thermal study of different compositions reveals that there are three reactions of

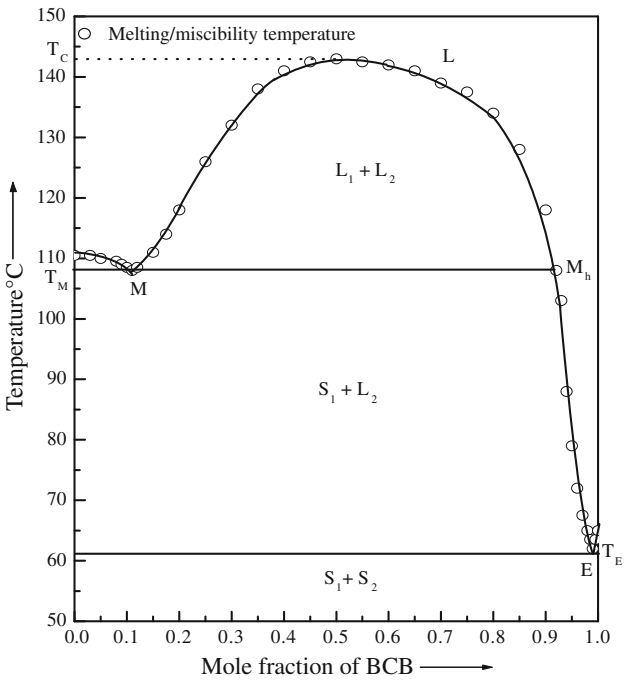

Fig. 1 Phase diagram of 4-bromochlorobenzene–resorcinol system. *Circle* melting/miscibility temperature

interest, which occur isothermally on solidification. The first reaction concerns the phase separation in two liquids as the single liquid phase, above 143.0 °C, is cooled below the critical temperature (T_c), and can be written as

$$L \leftrightarrow L_1 + L_2$$

The direct observation on kinetics of phase separation from liquid L to L_1 and L_2 is interesting but the explanation of mechanism is complicated. The disturbance in the whole liquid was observed which might be the consequence of diffusion, collision between droplets, convection, and movement by buoyancy driven fluid flow. A small decrease in temperature from the critical solution temperature (143.0 °C) is enough for the phase separation process to occur within few seconds. Although, in organic systems, the exact reason for the existence of miscibility gap is not clear, in the metallic systems the numbers of possibilities such as compound formation tendencies, atomic radii difference, valence differences of the component associating, etc. [20, 21] may be responsible for the occurrence of the miscibility gap in the liquid state. The intermolecular space and its variation with temperature as well as the intra and intermolecular forces may be the other possible reasons for miscibility gap in organic compounds. The second reaction, known as monotectic reaction, is quite similar to the eutectic reaction except that one of the product phases is a second liquid L_2, as follows:

$$L_1 \leftrightarrow S_1 + L_2$$

The third reaction is the eutectic reaction in which the liquid L_2 decomposes to give two solids as

$$L_2 \leftrightarrow S_1 + S_2$$

The monotectic, the eutectic, and the critical solution temperatures in the present case are 108.0, 62.0, and 143.0 °C, respectively. The monotectic and the eutectic points are the invariant points.

Growth kinetics

In order to study the crystallization behaviour of the pure components, the eutectic and the monotectic the crystallization rate (v) have been determined at different undercoolings (ΔT) by measuring the rate of movement of solid–liquid interface in a capillary. The plots between log ΔT and log v, for different materials, are given in Fig. 2 and the linear dependence of these plots are in accordance with Hillig and Turnbull [22] equation

$$v = u(\Delta T)^n \quad (1)$$

where u and n are constants and depend on the solidification behaviour of the materials involved. The experimental values of these constants are given in Table 1. The value of u for the monotectic is greater than those of their pure components, and for the eutectic it is less than the pure components. These results may be explained on the basis of the mechanism proposed by Winegard et al. [23]. According to this, in a binary system, eutectic/monotectic crystallization begins with the formation of a nucleus of one of the phases. The phase with metallic behaviour or with higher melting point one will start nucleating first and it will grow until the surrounding liquid becomes rich in the other component and a stage is reached when the second component also starts nucleating. Now there are two possibilities, either the two initial crystals may grow side-by-side or there may be alternate nucleation of the two phases. It is evident from the Table 1 that the crystallization velocity of the monotectic is more than the pure components and explains the alternate nucleation process of two phases involved. On the other hand, the rate of crystallization of the eutectic is less than the rate of crystallization of the pure components. The two phases of eutectic solidify and grow side-by-side mechanism.

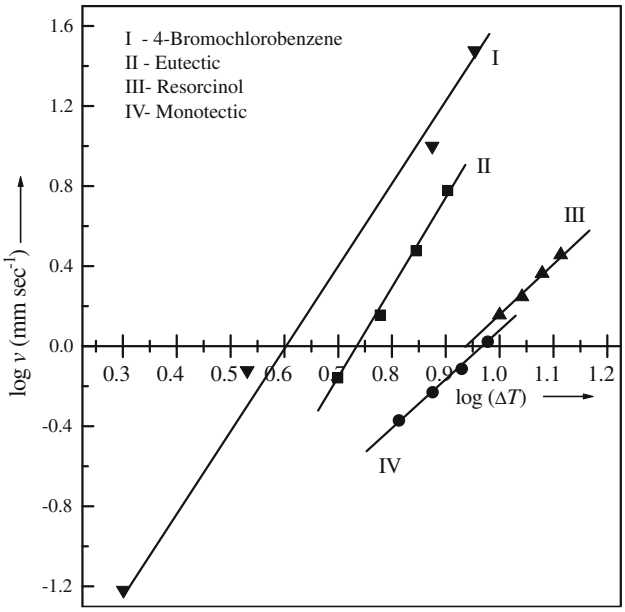

Fig. 2 Linear velocity of crystallization at various undercooling for 4-bromochlorobenzene, resorcinol and their monotectic and eutectic

Thermochemistry

Enthalpy of fusion

The values of enthalpy of fusion of the pure components, the eutectic and the monotectic are determined by the DSC method and have been reported in Table 1. For comparison, the value of enthalpy of fusion of eutectic calculated by the mixture law [17] is also included in the same table.

Table 1 Heat of fusion, entropy of fusion, roughness parameter and values of u and n for pure components, monotectic and eutectic

Materials	Heat of fusion (kJ mol^{-1})	Entropy of fusion (J mol^{-1} K^{-1})	Roughness parameter (α)	u (mm s^{-1} deg^{-1})	n
BCB	19.90	58.90	7.08	2.92×10^{-3}	2.68
R	22.20	57.90	6.96	4.56×10^{-3}	3.94
Monotectic	22.25	58.40	7.02	5.11×10^{-3}	2.36
Eutectic (Exp.)	16.98	50.70	6.10	4.08×10^{-4}	4.59
(Cal.)	19.92				

The enthalpy of mixing which is the difference of experimentally determined and the calculated values of the enthalpy of fusion are found to be -2.94 kJ mol^{-1}. From enthalpy of mixing, three types of structures are suggested [18]; quasi-eutectic for $\Delta_{mix}H > 0$, clustering of molecules for $\Delta_{mix}H < 0$ and the molecular solution for $\Delta_{mix}H = 0$. The negative value of $\Delta_{mix}H$ for the eutectic suggests the cluster structure in the binary melt of the eutectic. The entropy of fusion ($\Delta_{fus}S$) values, for different materials has been calculated by dividing the enthalpy of fusion by their corresponding absolute melting temperatures (Table 1). The positive values suggest that the entropy factor favours the melting process. The entropy of fusion value of eutectic is less than that of the parent components which shows that randomness of the eutectic composition is relatively low and infers the more stability of eutectic.

Size of critical nucleus and interfacial energy

When liquid is cooled below its melting temperature, it does not solidify spontaneously, because under equilibrium condition the melt contains number of clusters of molecules of different sizes. As long as the clusters are well below the critical size, they cannot grow to form crystals, and no solid would result. The critical size (r^*) of nucleus [18] is related to interfacial energy (σ) by the equation,

$$r^* = \frac{2\sigma T_{fus}}{\Delta_{fus}H.\Delta T} \tag{2}$$

where T_{fus}, $\Delta_{fus}H$, and ΔT are melting temperature, heat of fusion, and degree of undercooling, respectively. An estimate of the interfacial energy [16] is given by the expression

$$\sigma = \frac{C.\Delta_{fus}H}{(N_A)^{1/3}.(V_m)^{2/3}} \tag{3}$$

where N_A is the Avogadro number, V_m is the molar volume, and parameter C lies between 0.30 and 0.35. The calculated values of critical nucleus at different undercoolings and interfacial energy for different materials are reported in Tables 2 and 3, respectively.

Table 2 Critical radius of BCB, R and their monotectic and eutectic

Undercooling ΔT (°C)	Critical radius $\times 10^8$ cm			
	R	BCB	Monotectic	Eutectic
2.0		5.660		
3.4		3.330		
5.0				0.026
6.0				0.022
6.5			0.063	
7.0				0.019
7.5		1.510	0.055	
8.0				0.017
8.5			0.049	
9.0		1.260		
9.5			0.043	
10.0	1.630			
11.0	1.481			
12.0	1.360			
13.0	1.250			

Table 3 Interfacial energy of BCB, R and their eutectic and monotectic

Parameter	Interfacial energy $\times 10^6$ (kJ m^{-2})
σ_{SL_1} (R)	47.17
σ_{SL_2} (BCB)	33.30
$\sigma_{L_1L_2}$ (BCB–R)	1.20
σ_E (BCB–R)	33.44

Excess thermodynamic functions

The deviation from the ideal behaviour can best be expressed in terms of excess thermodynamic functions, namely, excess free energy (g^E), excess enthalpy (h^E), and excess entropy (s^E) which give a more quantitative idea about the nature of molecular interactions. The excess thermodynamic functions [18] could be calculated by using the following equations and the values are given in Table 4.

Table 4 Excess thermodynamic functions for the eutectic

Material	g^{E} (kJ mol^{-1})	h^{E} (kJ mol^{-1})	s^{E} (kJ mol^{-1} K^{-1})
Eutectic	−0.04	−13.080	−0.039

$$g^{E} = RT\left[x_1 \ln\gamma_1^{l} + x_2 \ln \gamma_2^{l}\right] \tag{4}$$

$$h^{E} = -RT^2\left[x_1\frac{\partial \ln \gamma_1^{l}}{\partial T} + x_2\frac{\partial \ln \gamma_2^{l}}{\partial T}\right] \tag{5}$$

$$s^{E} = -R\left[x_1 \ln\gamma_1^{l} + x_2 \ln \gamma_2^{l} + x_1 T\frac{\partial \ln \gamma_1^{l}}{\partial T} + x_2 T\frac{\partial \ln \gamma_2^{l}}{\partial T}\right] \tag{6}$$

where γ_i^{l}, x_i, and $\frac{\partial \ln \gamma_i^{l}}{\partial T}$ are activity coefficient in liquid state, the mole fraction and variation of log of activity coefficient in liquid state as function of temperature of component i.

It is evident from Eqs. 4–6 that activity coefficient and its variation with temperature are required to calculate the excess functions. Activity coefficient (γ_i^{l}) could be evaluated [24] by using the equation

$$-\ln\left(x_i\gamma_i^{l}\right) = \frac{\Delta_{\text{fus}}H_i}{R}\left(\frac{1}{T_E} - \frac{1}{T_i}\right) \tag{7}$$

where x_i, $\Delta_{\text{fus}}H_i$, T_i, and T_E are mole fraction, enthalpy of fusion, melting temperature of component i and eutectic melting temperature, respectively. The variation of activity coefficient with temperature could be calculated by differentiating Eq. 7 with respect to temperature

$$\frac{\partial \ln \gamma_i^{l}}{\partial T} = \frac{\Delta_{\text{fus}}H_i}{RT^2} - \frac{\partial x_i}{x_i \partial T} \tag{8}$$

$\partial x_i/\partial T$, in this expression can be evaluated by taking two points near the eutectic. The negative value of excess free energy, g^{E}, suggests that the interactions between unlike molecules are stronger than those between like molecules [24].

Microstructure

It is well known that in polyphase materials the microstructure gives information about shape and size of the crystallites, which play a very significant role in deciding about mechanical, electrical, magnetic, and optical properties of materials. The growth morphology [25] of a eutectic system is controlled by the growth characteristics of the constituent phases. According to Hunt and Jackson [26] the type of growth from melts depends upon the interface roughness (α) defined by

$$\alpha = \xi\Delta_{\text{fus}}H/RT \tag{9}$$

where ξ is a crystallographic factor which is generally equal to or less than one. The values of α are reported in Table 1. If $\alpha > 2$ the interface is quite smooth and the crystal develops with a faceted morphology. On the other hand, if $\alpha < 2$, the interface is rough and many sites are continuously available and the crystal develops with a non-faceted morphology.

Microstructure of monotectic

In monotectic solidification when liquid of monotectic composition (Fig. 1) is allowed to cool, below the monotectic temperature (T_M), the stability of two liquid phases L_1, L_2 and a solid phase S at the solid–liquid interface are required. The necessary conditions for the stability of three phases in contact have been explained by Chadwick [27]. Whether droplets nucleate in the melt or on the solid–liquid interface depends on the relative magnitude of the three interfacial energies. The requirement for the balance of interfacial energies is given by the conditions:

$$\sigma_{SL_2} \leq \sigma_{SL_1} + \sigma_{L_1L_2} \tag{10}$$

and

$$\sigma_{SL_2} \geq \sigma_{SL_1} + \sigma_{L_1L_2} \tag{11}$$

where σ_{SL_1}, σ_{SL_2}, and $\sigma_{L_1L_2}$ are the interfacial energies of solid S and the liquid L_1, solid S and the liquid L_2, and liquids L_1 and liquid L_2, respectively. The surface energies were calculated by using the equation reported earlier [15, 16], and have been tabulated in Table 3. The Cahn wetting condition [28] could be successfully applied to the present system as the interfacial energies are related by

$$\sigma_{SL_2} < \sigma_{SL_1} + \sigma_{L_1L_2}$$

which is indicating that the BCB–R liquid (L_1) wets the solidified BCB perfectly. The unidirectional solidify optical microphotographs of monotectic (Fig. 3a, b), show the solidification features of monotectic alloy. The rapidly solidify microstructure (Fig. 3a) shows the tendency of lamella formation with elongated spherical shape of droplets while slow rate solidify microstructure (Fig. 3b) shows well arranged and equidistant array of spherical droplets in a particular direction. In Fig. 3b the BCB has got sufficient time to form the droplets.

Microstructure of the eutectic

The thermal gradient could not be maintained unidirectional during the growth of microstructure of eutectic (Fig. 3c). The middle part of the structure, which has unidirectional temperature gradient, shows broken lamellar and elongated droplets. To have minimum surface energy, the tendency of liquid phase is to acquire the spherical shape and it depends on the availability of time. The elongated spherical structures are frequently observed if

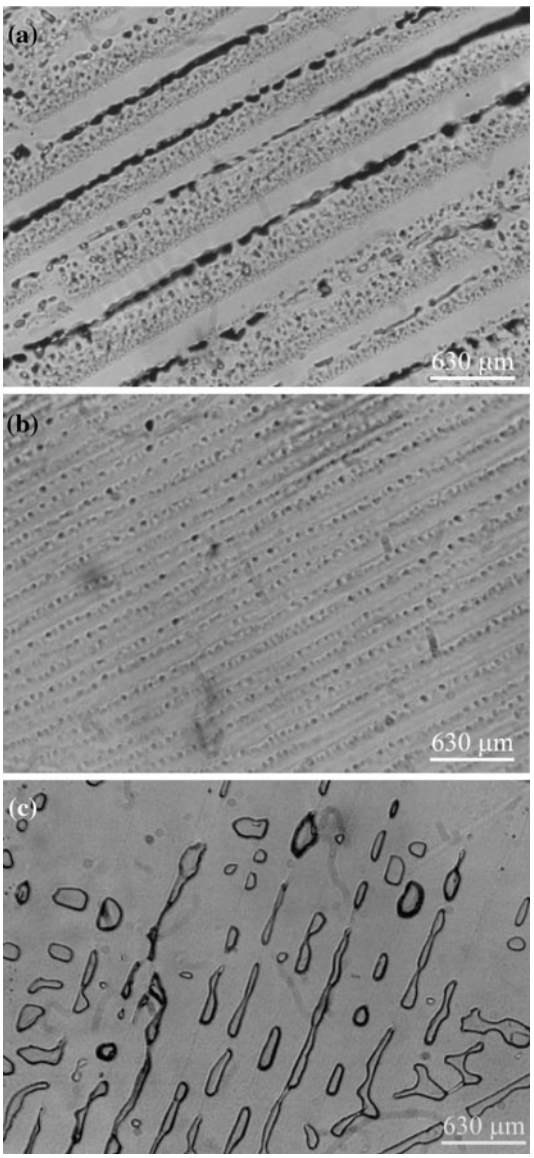

Fig. 3 Directionally solidify optical microphotograph of 4-bromochlorobenzene–resorcinol monotectic (**a** and **b**), and eutectic (**c**)

time of formation of sphere is more than the freezing time of other phase.

Conclusions

The experimentally determined phase diagram of 4-bromochlorobenzene–resorcinol shows the formation of a eutectic and a monotectic where the mole fraction of BCB are 0.99 and 0.11, respectively. The consolute temperature was found to be 35.0 °C above the monotectic horizontal. The growth kinetics of pure components, the eutectic and the monotectic determined at different undercoolings suggest that growth takes place according to the Hillig–Turnbull equation. The entropy of fusion, enthalpy of mixing, excess thermodynamic functions and interfacial energy were computed using the enthalpy of fusion values determined by the DSC method. The negative value of $\Delta_{mix}H$ for the eutectic suggests the cluster structure in the binary melt of the eutectic, while the relation of interfacial energies, $\sigma_{SL_2} < \sigma_{SL_1} + \sigma_{L_1L_2}$, confirm the applicability of Cahn wetting condition to the present system. Microstructural investigations of eutectic and monotectic show broken lamella and well arranged array of droplets.

Acknowledgements Authors sincerely thank the Board of Research in Nuclear Science, Department of Atomic Energy, Mumbai, India for financial support and to the Head of the Department of Chemistry, B.H.U. Varanasi, for providing infrastructure facility. Mr. K. P. Sharma also thanks Tribhuvan University (Nepal) for providing study leave and UGC (Nepal) for Research Fellowship.

References

1. George F, Voort V (1998) Mater Char 41:69
2. Herlach DM, Cochrane RF, Egry IH, Fecht J, Greer AL (1993) Int Mater Rev 38:273
3. Savas MA, Erturan H, Altintas S (1997) Metall Mater Trans 28A:1509
4. Mazumdar B, Chattopadhyay K (2000) Metall Mater Trans 31A:1833
5. Labie R, Ruythooren W, Humbeeck JV (2007) Intermetallics 15:396
6. Rosenthal Y, Stern A, Cohen SR, Eliezer D (2010) Mater Sci Eng A 527:4014
7. Kaukler WF, Frazier DO (1986) Nature 323:50
8. Rai RN, Lan CW (2002) J Mater Res 17:1587
9. Kant S, Reddi RSB, Rai RN (2010) Fluid Phase Equilib 291:71
10. Gunter P (2000) Nonlinear optical effects and materials. Springer-Verlag, Berlin
11. Smirani I, Auban-Senzier P, Jerome D, Brau A, Farges JP (1999) Synth Met 102:1259
12. Rai RN (2004) J Mater Res 19:1348
13. Singh NB, Agrawal T, Gupta P, Das SS (2009) J Chem Eng Data 54:1529
14. Bassi PS, Sharma RP (1996) Indian J Chem 35A:133
15. Reddi RSB, Shiva K, Rai US, Rai RN (2009) J Cryst Growth 312:95
16. Sharma KP, Reddi RSB, Shiva K, Rai RN (2010) Thermochim Acta 498:112
17. Rai US, Rai RN (1996) J Cryst Growth 169:563
18. Rai RN, Rai US, Verma KBR (2002) Thermochim Acta 387:101
19. Dodd JW, Tonge KH (1987) In: Currel BR (ed) Thermal methods, analytical chemistry by open learning. Willey, New York, p 120
20. Ratke L, Diefenbach S (1995) Mater Sci Eng R15:263
21. Predel B (1997) J Phase Equilib 18:327
22. Hillig WB, Turnbull DJ (1956) J Chem Phys 24:914
23. Winegard WC, Majka S, Thall BM, Chalmers B (1957) Can J Chem 29:320
24. Rai US, Rai RN (1998) J Therm Anal 53:883
25. Elliot R (1977) Int Metals Rev 22:161
26. Hunt JD, Jackson KA (1966) Trans Met Soc AIME 236:843
27. Chadwick GA (1972) Metallography of phase transformations. Butterworth, London, p 312
28. Cahn JW (1977) J Chem Phys 66:3667